Supporting Information

Large-Area Layer Counting of Two-Dimensional Materials Evaluating the Wavelength Shift in Visible-Reflectance Spectroscopy

Andreas Hutzler[1,], Christian D. Matthus[2], Christian Dolle[3], Mathias Rommel[2], Michael P. M. Jank[2], Erdmann Spiecker[3], Lothar Frey[1,2]*

[1] Electron Devices (LEB), Department of Electrical, Electronic and Communication Engineering, Friedrich-Alexander-University Erlangen-Nürnberg (FAU), Cauerstraße 6, 91058 Erlangen, Germany

[2] Fraunhofer Institute for Integrated Systems and Device Technology IISB, Schottkystraße 10, 91058 Erlangen, Germany

[3] Institute of Micro- and Nanostructure Research (IMN) & Center for Nanoanalysis and Electron Microscopy (CENEM), Department of Materials Science and Engineering, Friedrich-Alexander-University Erlangen-Nürnberg (FAU), Cauerstraße 3, 91058 Erlangen, Germany

*corresponding author

Email: andreas.hutzler@leb.eei.uni-erlangen.de

ORCID: https://orcid.org/0000-0001-5484-707X

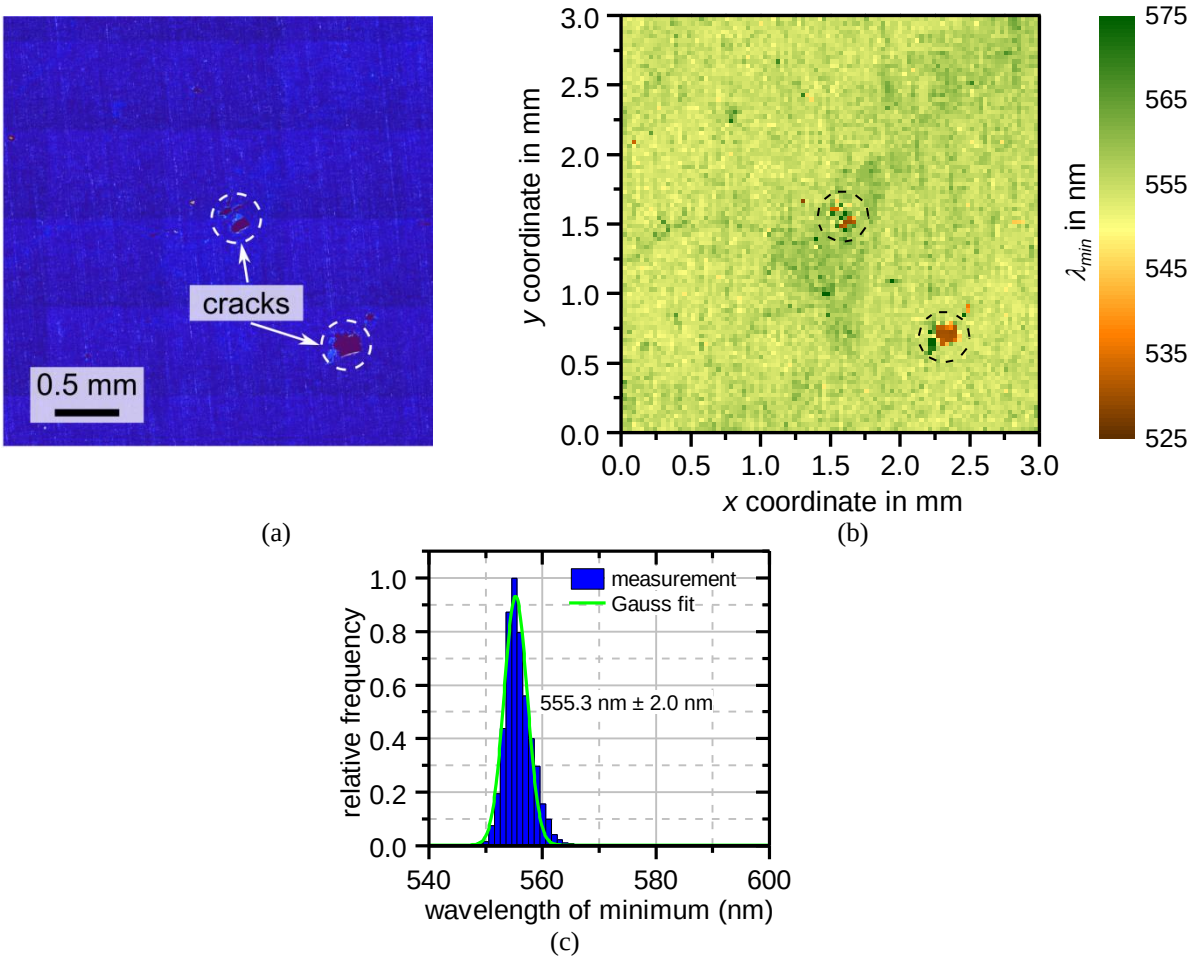

Figure S1. *(a) Optical micrograph of 3-5 layer graphene, (b) map of the reflectance minima for (a). Two characteristic cracks are highlighted in (a) and (b). (c) spectral distribution of the reflectance minima (10,000 spectra recorded).*

The graphene coated samples G1 and G2 were investigated using SEM. The results are shown in **Figure S2**. In this figure the inhomogeneous island structure is clearly visible. Furthermore, wrinkles and particles can be seen. These can be identified in an AFM micrograph which was acquired on single-layer graphene on the used optical layer stack shown in **Figure S3** as well.

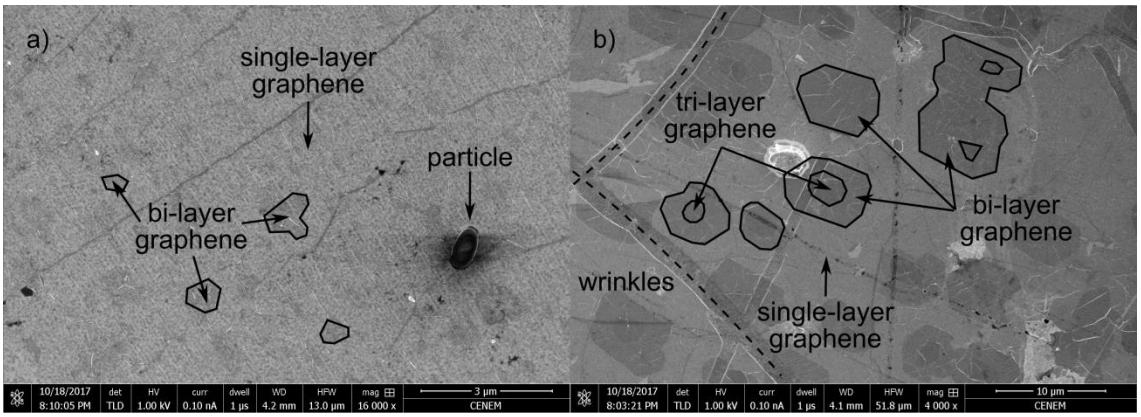

Figure S2. *SEM micrographs of (a) single-layer graphene (sample G1) and (b) bi-layer graphene (sample G2). Some islands of single-layer, bi-layer, and tri-layer graphene are highlighted in both figures verifying the island structure of CVD graphene grown on Cu substrate.*

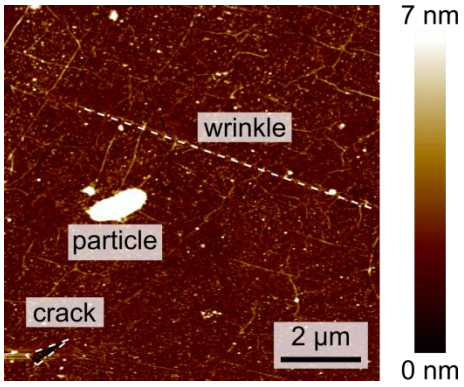

(c)

Figure S3. *AFM micrograph of single-layer graphene with PMMA residuals. The huge particle was not considered for roughness determination of the sample.*

TEM measurements (diffraction and imaging) were performed. Diffraction patterns of single-layer graphene (sample G1) and bi-layer graphene (sample G2) are shown in **Figure S4(a)** and **Figure S4(c)**, respectively. Corresponding peak intensities in the diffraction patterns are shown in **Figure S4(b)** and **Figure S4(d)**, respectively. In the case of single-layer graphene the peak intensities of reflexes which arise due to scattering at {0-110} planes are identical to those of {1-210} planes. In the case of bi-layer graphene the reflexes which arise due to scattering at {1-210} planes are significantly larger than those of {0-110} planes [8]. This is clearly visible in **Figure S4(d)** and gives evidence for the presence of single-layer and bi-layer graphene.

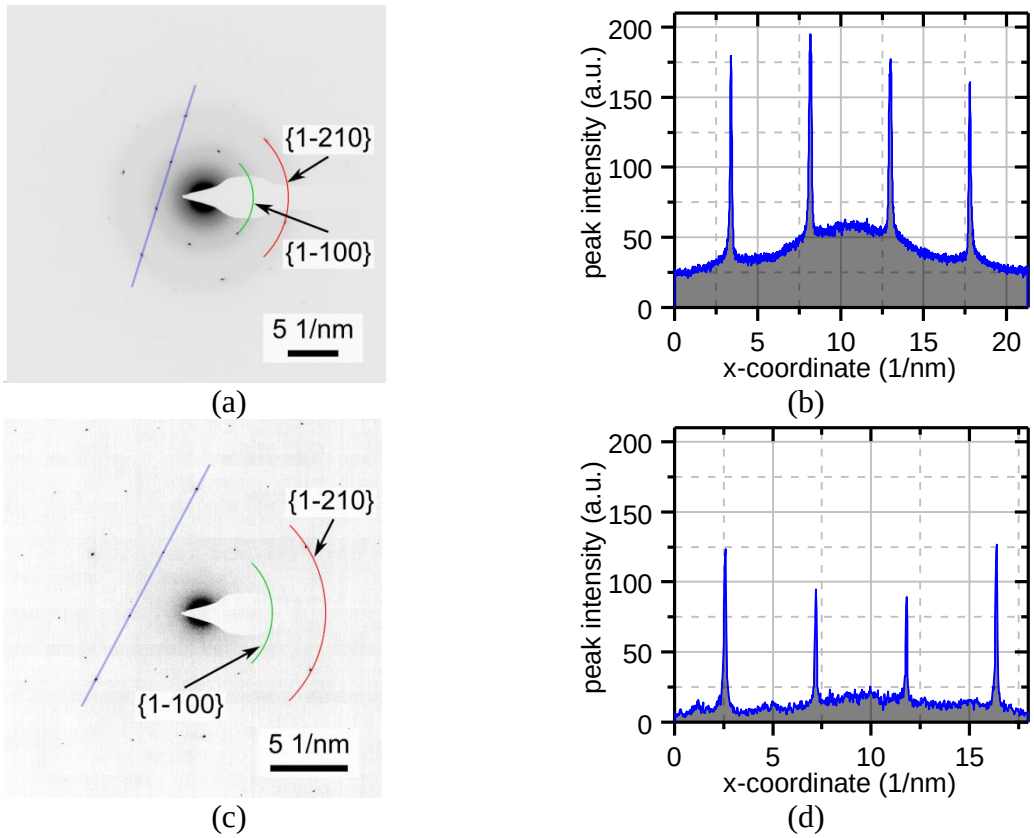

Figure S4. *TEM SAED patterns of (a) single-layer graphene with (b) corresponding peak intensities of the indicated peaks, (c) SAED pattern of bi-layer graphene with (d) corresponding peak intensities of the indicated peaks.*

Furthermore, sample G6/8 was investigated by HAADF STEM. Results are shown in **Figure S5(a)**. The island-like structure of the few-layer graphene can be seen in a micrograph that was recorded using a high-angle annular dark field detector during scanning TEM (**Figure S5(a)**). The TEM selected area electron diffraction (SAED) pattern (**Figure S5(b)**) shows a strong rotation of the single layers. This is caused by the turbostratic structure of the grown graphene. Additionally, HRTEM investigations were performed on a FIB cross section of sample G6/8 (**Figure S5(c)**). These investigations confirm the thicknesses of SiO_2 and Si_3N_4 of 10.8 nm ±0.2 nm and 53.5 nm ±0.5 nm, respectively. Furthermore, the number of layers can be directly determined at individual positions (**Figure S5(d)**). A mean number of layers of 9.7 with a standard deviation of 5.4 layers was determined at 236 different positions within the length of the cross section of approximately 7 µm. This high standard deviation shows the strong variations of the number of layers. However, the mean value differs from the optically measured number of layers of 6 ± 0.6 as the HRTEM investigations are only performed at small cross sections and are thus not directly comparable to the large-area measurements conducted with the optical method.

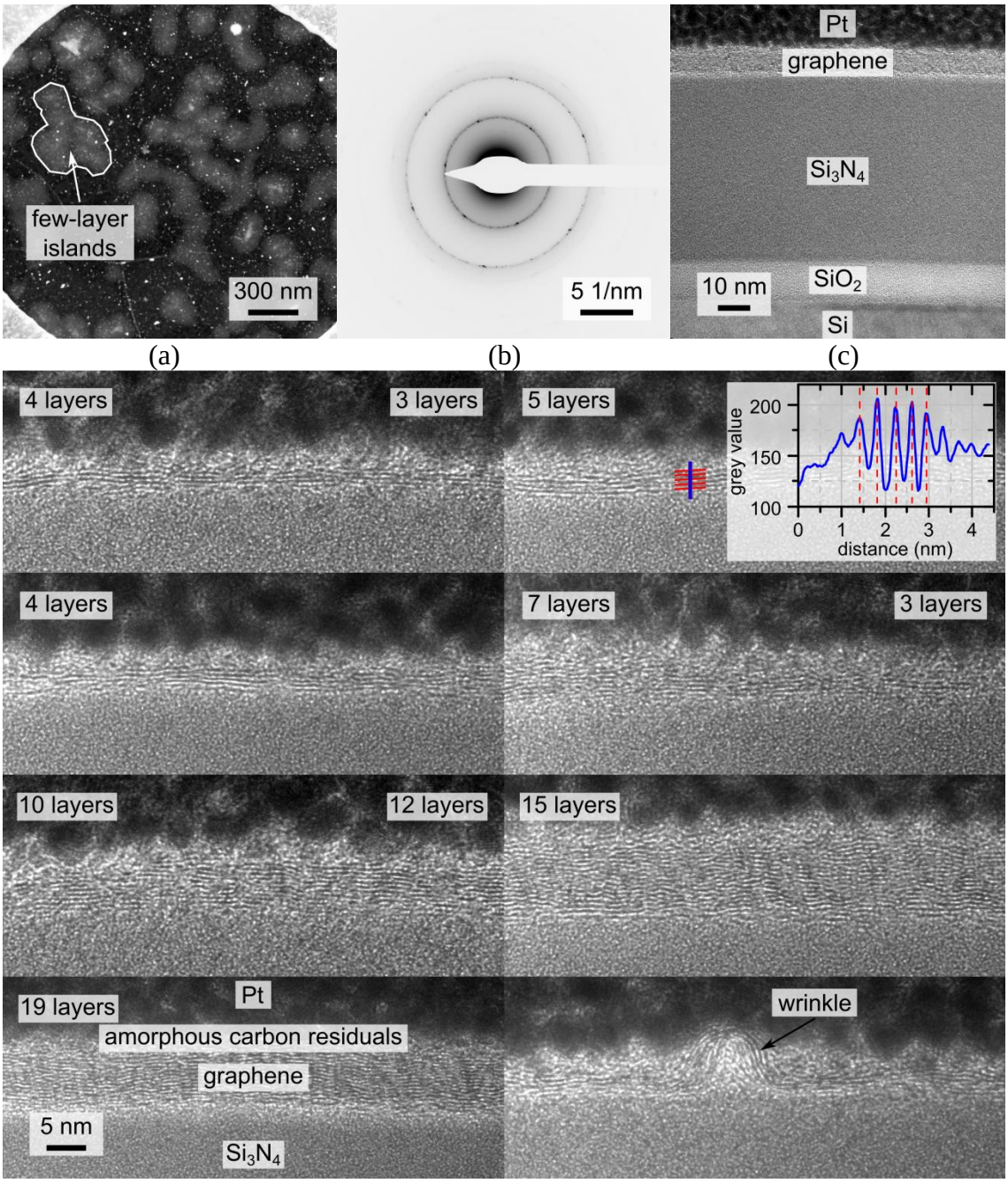

Figure S5. *(a) HAADF STEM micrograph,(b) SAED pattern from sample G6/8, (c) and (d) overview and individual positions of the layer stack investigated by HRTEM of a FIB cross section of sample G6/8.*

A layer stack consisting of SiO_2 of a variable thickness on a Si substrate may also be utilized for the determination of atomic layers of TMDs. In this case, the second and the third minimum are used. The reflectance, the minimum wavelength for 0 layers and for 10 layers, the wavelength shift and the coefficient of determination are shown over the SiO_2 layer thickness for MoS_2, $MoSe_2$, and $MoTe_2$, respectively in **Figure S6**.

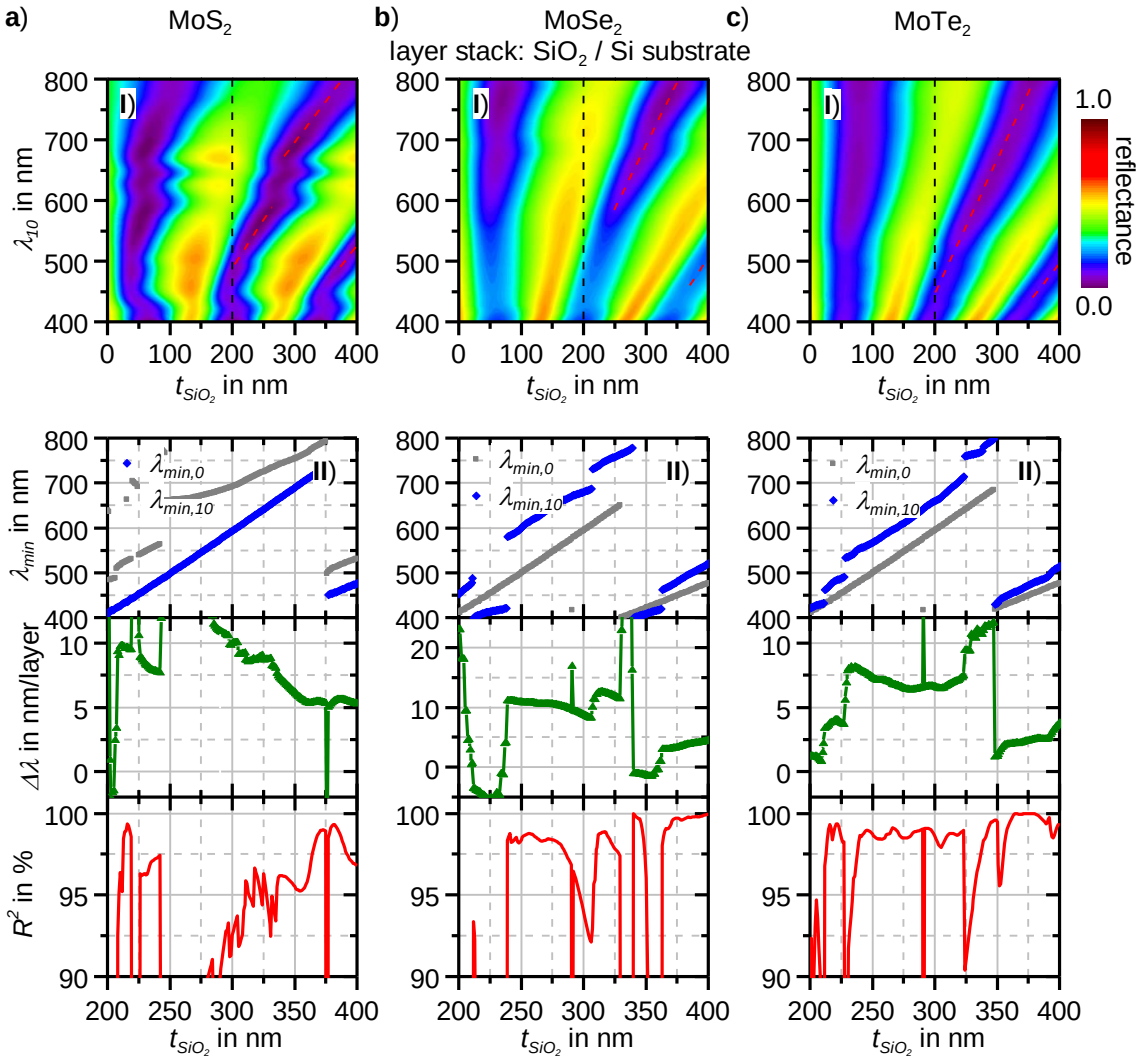

Figure S6. *I) Reflectance plots of 10 layers (a) MoS_2, (b) $MoSe_2$, and (c) $MoTe_2$ on SiO_2 on Si substrate for different SiO_2 thicknesses. II) Top: wavelength of reflectance minimum of the substrate without and with 10 layers of 2D material (i.e., $\lambda_{min,0}$ and $\lambda_{min,10}$, respectively), center: wavelength shift per layer, and bottom: coefficient of determination.*

For the utilization of the introduced method for other 2D materials their optical properties have to be considered. Therefore, the spectral complex refractive indices of materials used for the calculations in this work are depicted in **Figure S7** (layer stack) and **Figure S8** (2D materials). In the latter figure oscillator frequencies are highlighted.

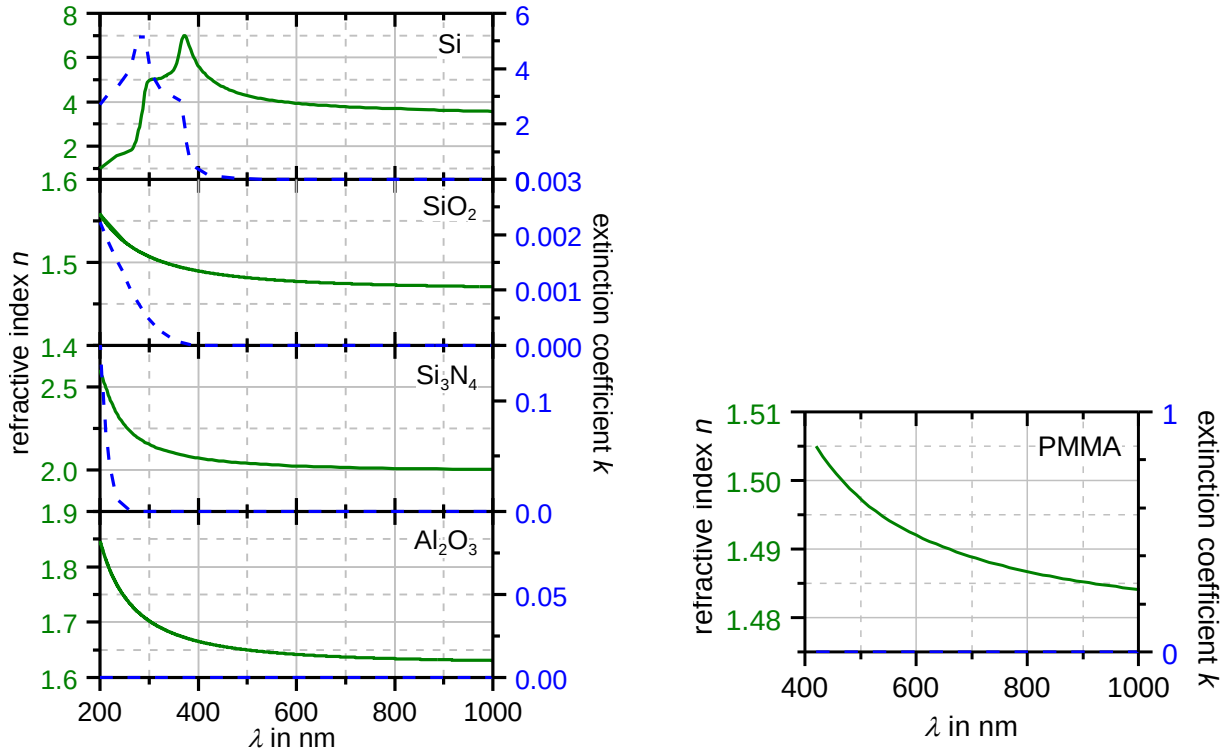

Figure S7. *(a) Spectral refractive index (solid line) and extinction coefficient (broken line) used for the calculations in this work of Si [S1], SiO_2 [S2], Si_3N_4 [S3], and Al_2O_3 (note: the extinction coefficient of Al_2O_3 was assumed to be below 10^{-5} within the considered wavelength range [45]) and (b) complex refractive index of PMMA [S4].*

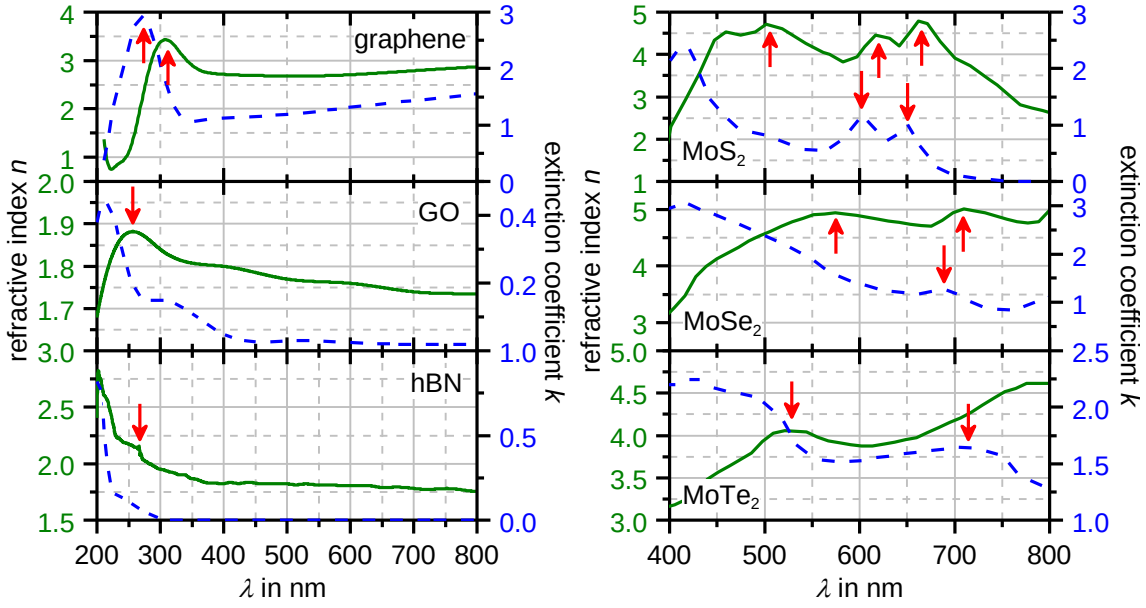

Figure S8. *Spectral refractive index (solid line) and extinction coefficient (broken line) used for the calculations in this work of graphene [S5], GO [47], hBN [49], MoS_2 [52], $MoSe_2$ [51], and $MoTe_2$ [51]. Oscillator frequencies highlighted by red arrows.*

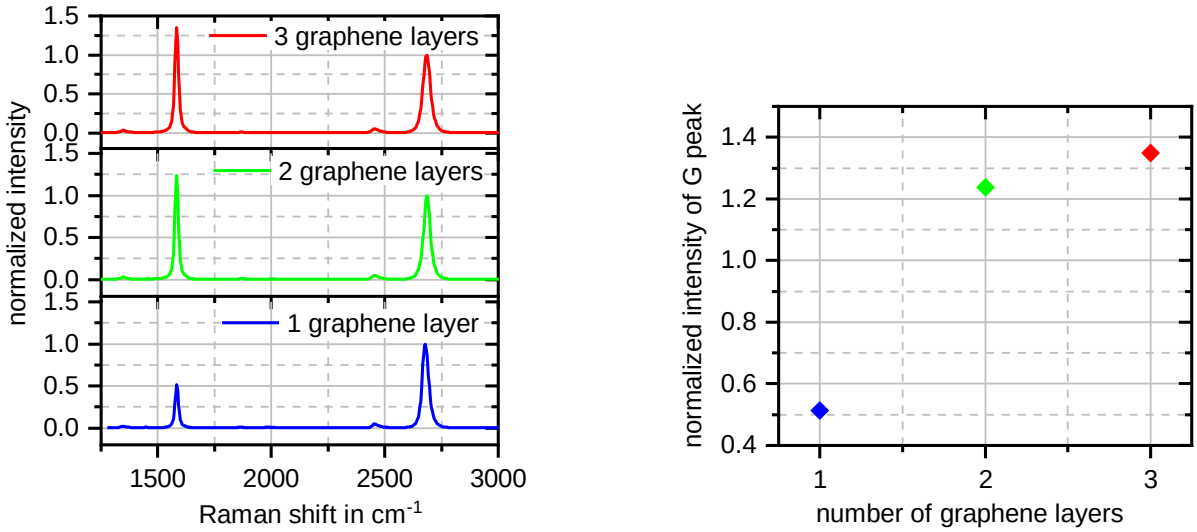

Figure S9. *(a) Raman spectra of one to three layers of graphene and (b) normalized intensity of G peak.*

References Supporting Information

[S1] Vuye G *et al.* 1993 *Thin Solid Films* **233** 166-70.

[S2] Gao L, Lemarchand F, and Lequime M 2013 *J. Europ. Opt. Soc. Rap. Public.* **8** 13010.

[S3] Philipp H R 1973 *J. Electrochem. Soc.* **120** 295-300.

[S4] Beadie G *et al.* 2015 *Appl. Opt.* **54**, F139-F143.

[S5] Weber J W, Calado V E and van de Sanden M C M 2010 *Appl. Phys. Lett.* **97** 91904.